

A Measurement of Gamow-Teller Strength for $^{176}\text{Yb} \rightarrow ^{176}\text{Lu}$ and the Efficiency of a Solar Neutrino Detector

M. Bhattacharya^{1,2,3,a}, C. D. Goodman¹, R. S. Raghavan⁴, M. Palarczyk^{5,b}, A. García², J. Rapaport⁵, I. J. van Heerden^{1,c} and P. Zupranski⁶

¹*Indiana University Cyclotron Facility, Bloomington, Indiana 47408, USA*

²*University of Notre Dame, Notre Dame, Indiana 46556, USA*

³*Nuclear Physics Laboratory, University of Washington, Seattle, Washington 98195, USA*

⁴*Bell Laboratories, Lucent Technologies, Murray Hill, New Jersey 07974, USA*

⁵*Ohio University, Athens, Ohio 45701, USA*

⁶*The Andrzej Soltan Institute for Nuclear Studies, 00-689 Warsaw, Poland*

(November 20, 2018)

Abstract

We report a $0^\circ \text{ } ^{176}\text{Yb}(p, n)^{176}\text{Lu}$ measurement at IUCF where we used 120 and 160 MeV protons and the energy dependence method to determine GT matrix elements relative to the Fermi matrix element which can be calculated model independently. The data show that there is an isolated concentration of GT strength in the low lying 1^+ states making the proposed Low Energy Neutrino Spectroscopy (*LENS*) detector (based on neutrino captures on ^{176}Yb) sensitive to ^7Be and pp neutrinos and a promising detector to resolve the solar neutrino problem.

25.55.Kr, 26.65.+t, 27.70.+q

Typeset using REVTeX

I. MOTIVATION

The existing solar neutrino detectors are sensitive to different but overlapping regions of the solar neutrino spectrum. Combined data from these detectors have been used to estimate the individual contributions from the pp , ${}^7\text{Be}$ and ${}^8\text{B}$ neutrinos to the total solar neutrino flux. According to the present data the low energy pp neutrinos seem to be present in full strength compared to the solar model prediction. The intermediate energy ${}^7\text{Be}$ neutrinos seem to be missing entirely, while only about half of the high energy ${}^8\text{B}$ neutrinos are observed. This energy dependent suppression of the solar neutrino spectrum is known as the modern *solar neutrino problem*. There is a general consensus in the community that this energy dependent deficit of solar neutrinos cannot be explained by any reasonable modification of the solar model [1]. The most plausible solution appears to be an energy dependent conversion of solar ν_e 's to other flavors inside the Sun, *aka*, the MSW effect [2–5]. This idea can be fully tested only if the individual fluxes of at least pp and ${}^7\text{Be}$ neutrinos can be measured.

The Low Energy Neutrino Spectroscopy (*LENS*) detector proposed recently by Raghavan [6] will use a low-threshold, real-time, flavor-specific (using charged current neutrino capture) detection scheme based on Gamow-Teller (GT) transitions from ${}^{176}\text{Yb} \rightarrow {}^{176}\text{Lu}$ for directly measuring the ${}^7\text{Be}$ and the pp neutrino flux. The ${}^7\text{Be}$ ν_e flux measured by *LENS* along with the results from the *BOREXINO* [7] detector (sensitive to all flavors of ${}^7\text{Be}$ neutrinos) will provide direct evidence of *Solar Neutrino Flavor Oscillation*. In addition *LENS* also promises to be the first detector capable of directly measuring the pp neutrino flux.

In order to estimate the neutrino capture event rates for this detector one needs an

^aE-mail:mbhattac@marie.npl.washington.edu

^bPermanent address: Henryk Niewondniczański Institute of Nuclear Physics, 31-342 Kraków, Poland.

^cPermanent address: University of Western Cape, Bellville, South Africa.

accurate knowledge of the weak interaction matrix elements for the transitions from the ground state of ^{176}Yb to the two low-lying levels in ^{176}Lu . We report here a charge exchange reaction $[0^\circ (p, n)]$ measurement of these matrix elements.

II. EXPERIMENT

At IUCF we measured $^{176}\text{Yb}(p, n)^{176}\text{Lu}$ at 0° using the IUCF neutron time-of-flight (*NTOF*) system in spectroscopy mode, with 120 and 160 MeV protons. We used a procedure, described in Refs. [8,9], in which the incident proton energy dependence of the ratio of the specific GT to the specific Fermi cross section is exploited to determine from the spectra the GT matrix elements relative to the model independent Fermi matrix element. It is a well known fact that all of the Fermi strength resides in the isobaric analog state transition, which is clearly seen as a sharp peak in (p, n) spectra. The use of the energy dependence method allows us to avoid the large uncertainties (as pointed out in Ref. [8]) involved in using globally averaged reaction cross section on a single spectrum. Fig. 1(a) and (b) show the low energy part of the missing mass spectrum for 120 MeV and 160 MeV protons respectively. The data show that there is an isolated concentration of GT strength in the low-lying 1^+ states.

The level scheme of ^{176}Yb indicates that there are two 1^+ levels, not resolved in (p, n) but resolved in a complementary $(^3\text{He}, t)$ experiment at Osaka [10], in this region of concentrated GT strength. For *LENS* to be able to detect the pp neutrinos it is essential that the lower excitation energy state contain a significant portion of this GT strength. Although the two low lying states were not physically resolved in our measurement, it is possible to separate the GT strengths to the two states by fixing the peak shape parameters to their accurately determined values from an auxiliary spectrum (described below) and by fixing the excitation energies of the two states to their well known values. Accurate peak shape knowledge is also needed to determine precisely the number of counts in the Fermi peak used in normalizing the spectra to $B(\text{GT})$.

A. Peak shape Analysis

Neutron time of flight peak shapes are determined by the response of the detection system and the convoluted energy-time profile of the proton beam bunch. An additional effect that contributes to the peak shape is the scattering of the neutrons by the ground below and near the detectors. Our empirical peak shape consists of a Gaussian (accounting for the detector response, the beam energy profile, and the primary time structure of the beam bunch) convoluted with a fast exponential on either side of the Gaussian to fully take into account the time structure of the beam bunch. To take into account the contribution to the peak shape by the neutrons scattered from the ground below the detectors a long (slow) exponential was also convoluted to the low neutron energy (high excitation energy) side of the Gaussian, as these neutrons traverse a longer path than the direct neutrons. As described in more detail in Ref. [9], the counts in this tail are not from the solid angle of the detector and should ideally be removed from the analysis.

In this experiment, however, we make use only of the relative areas of the peaks corresponding to the low-lying final states and the IAS. Using only relative peak areas eliminates systematic uncertainties involved in determining absolute cross sections. The uncertainty in a peak ratio resulting from an imperfect separation of direct peak from the tail is only second order due to a possible change in the direct to scattered ratio between the unknown GT transition and the IAS peak.

As we simply ascribe a functional form to the observed peak shapes rather than modeling them from first principles, it is extremely important to test our empirical peak shape and to obtain the best values for its free parameters from an auxiliary spectrum using the same experimental setup. We chose the $^{13}\text{C}(p, n)^{13}\text{N}$ reaction because of its well resolved level structure for this purpose. Our fit to the ^{13}N ground state using this peak shape and the Levenberg-Marquardt method is shown in Fig. 2. The fit shows that our peak shape describes the data very well. We used the peak shape parameters obtained from this peak to fit the ^{176}Lu spectrum shown in Fig. 1(a) and (b).

B. Transition Strengths

As described in detail in Refs. [8] and [9], the specific Fermi and GT cross sections have a strong mass number dependence that can not be accurately predicted by reaction dynamics theory. Hence the best way to normalize spectra to GT strengths is to normalize them to the Fermi transition. This procedure requires obtaining the number of counts in the Fermi peak which is usually not isolated or resolved from nearby and underlying GT transitions. We use the strong incident proton energy dependence of the ratio of the Fermi to GT specific cross sections to extract the number of counts in the Fermi peak. In this procedure we match spectra taken at two proton energies at a GT transition close to the Fermi peak and iteratively subtract a peak of appropriate shape from the Fermi peak in each spectrum, while minimizing a figure of merit defined to be the sum of squared differences between the two spectra. The only assumptions that go into this procedure are that the nearby peak corresponds to a pure GT transition and that the energy dependence of the ratio of specific cross sections is universal (*i.e.* no mass dependence).

In this case (see Fig. 3) the Fermi peak rides on top a smooth Gamow Teller Giant Resonance (GTGR). Although the GTGR does not have a smooth structure in lighter nuclei, one expects it to be so in heavier nuclei as in our case. As a result, in this case one can fit the entire region containing the Fermi peak and the GTGR using our empirical peak shape for the Fermi peak and approximating the GTGR shape by a Lorentzian function. Fig. 3(a) and (b) show our best fit ($\chi^2_{min}/\nu=1.2$) to this region for the 120 and 160 MeV spectrum respectively and we can see that this model describes the data very well.

We separated the GT strengths to the two states in ^{176}Lu by fixing in our fit the parameters of our empirical peak shape to their values obtained from the ^{13}N spectrum. We also fix the well known excitation energies of the two low lying states in ^{176}Lu . The resulting fit ($\chi^2/\nu=1.1$) is shown in Fig. 1. The GT strengths to the two states using the areas obtained from this fit and the area for the Fermi peak obtained from Fig. 3 is given in Table I.

III. NEUTRINO ABSORPTION CROSS SECTION ON ^{176}Yb

In the allowed approximation, the neutrino absorption cross section on ^{176}Yb is given by:

$$\sigma(E_\nu) = \frac{g_V^2}{\pi \hbar^4 c^3} \sum_i p_i W_i F(Z, W_i) \left(\frac{g_A}{g_V} \right)^2 B_i(GT) . \quad (1)$$

The sum runs over all ^{176}Lu daughter levels, g_V and g_A are the β -decay vector [13] and axial vector coupling constants respectively, p_i and W_i refer to the momentum and total energy of the outgoing electron, and $F(Z, W)$ accounts for the Coulomb distortion of the outgoing electron wave function. We computed $\sigma(E_\nu)$ for the neutrino-capture reactions using the B_i -values from our measurement. We calculated $F(Z, W)$ using our codes for F_0 and screening corrections and by interpolating Behrens and Jänecke's [14] L_0 value (their Table II) for finite-size corrections. Fig. 4 shows the ^{176}Yb ν -absorption cross section as a function of the neutrino energy.

Our integrated $^{176}\text{Yb}(\nu_e, e)^{176}\text{Yb}^*$ cross section over the standard (no neutrino oscillations) pp and ^7Be neutrino spectra is shown in Table I. *LENS* will also be a real time detector of supernova neutrinos and we obtain a total absorption cross section of $(5.57 \pm 0.83) \times 10^{-42} \text{ cm}^2$ for ν_e 's from a Fermi-Dirac energy distribution with $T = 3.2 \text{ MeV}$ (corresponding to $\langle E_{\nu_e} \rangle = 10 \text{ MeV}$).

IV. CONCLUSIONS

We measured the transition strengths of $^{176}\text{Yb} \rightarrow ^{176}\text{Lu}$ using $0^\circ (p, n)$ reactions. Our measurement indicates that this proposed detector will be sensitive to ^7Be and pp neutrinos making *LENS* a promising detector to help resolve the solar neutrino problem. The lowest state is sensitive to all solar neutrino sources including pp neutrinos while the next excited state is sensitive to all sources except pp neutrinos.

ACKNOWLEDGMENTS

We thank Bill Lozowski for preparing the rolled foil Yb target. The IUCF and OU researchers were supported by the US National Science Foundation, (NSF). The Notre Dame researchers were supported by the NSF and the Warren Foundation.

TABLES

TABLE I. GT strengths and neutrino capture cross sections for the two low-lying states in ^{176}Lu obtained from our spectra.

$E_x(\text{keV})$ [15]	B(GT)	$\sigma_\nu(10^{-45}) \text{ cm}^2$		
		pp	${}^7\text{Be}(0.384)$	${}^7\text{Be}(0.862)$
194.511 ± 0.008	0.22 ± 0.03	11.16 ± 1.53	3.35 ± 0.46	77.95 ± 10.69
338.982 ± 0.010	0.12 ± 0.02	-	-	33.11 ± 5.75

FIGURES

FIG. 1. Low energy part of the $^{176}\text{Yb}(p,n)^{176}\text{Lu}$ missing mass spectra, (a) using 120 MeV and (b) 160 MeV protons. Solid lines are composite fits to the spectra using the peak shape parameters obtained from ^{13}N spectra. Dashed lines show the individual peaks.

FIG. 2. Low energy part of the $^{13}\text{C}(p,n)^{13}\text{N}$ missing mass spectra, (a) using 120 MeV and (b) 160 MeV protons. Fit to the spectra using our empirical peak shape is shown. Peak shape parameters obtained from these spectra are used in the subsequent fit to the ^{176}Lu spectra.

FIG. 3. High energy part of the $^{176}\text{Yb}(p,n)^{176}\text{Lu}$ spectrum (a) using 120 MeV and (b) using 160 MeV protons. Overall fit to the spectra using the empirical peak shape for the IAS peak and a Lorentzian for the GTGR is shown.

FIG. 4. Neutrino capture efficiency of LENS as a function of incident neutrino energy.

REFERENCES

- [1] N. Hata and P. Langacker, Phys. Rev. **D 56**, 6107 (1997).
- [2] J. N. Bahcall, P. I. Krastev and A. Yu. Smirnov, Phys. Rev. **D 58**, 096016-1 (1998).
- [3] Peter Fisher, Boris Kayser and Kevin S. McFarland, Ann. Rev. Nucl. Part. Sci. **49**, 481 (1999).
- [4] Y. Fukuda *et al.*, Phys. Lett. **B 433**, 9 (1998).
- [5] J. N. Abdurashitov *et al.*, Phys. Rev. Lett. **83**, 4686 (1999).
- [6] R. S. Raghavan, Phys. Rev. Lett. **78**, 3618 (1997).
- [7] *Borexino at Gran Sasso: A Real Time Detector for Low energy Solar Neutrinos*, edited by G. Bellini and R. S. Raghavan (Unpublished).
- [8] T. N. Taddeucci, C. A. Goulding, T. A. Carey, R. C. Byrd, C. D. Goodman, C. Gaarde, J. Larsen, D. Horen and E. Sugarbaker, Nucl. Phys. **A 469**, 125 (1987).
- [9] Charles D. Goodman, Manojeeet Bhattacharya, Stewart D. Bloom, Maurice B. Aufderheide and Pawel Zupranski, Submitted to Nucl. Instr. Meth.
- [10] M. Fujiwara *et al.*, submitted to Phys. Rev. Lett.
- [11] W. H. Press, S. A. Teukolsky, W. T. Vetterling and B. P. Flannery, *Numerical Recipes*, Cambridge University Press (1992).
- [12] G. Audi and A.H. Wapstra, Nucl. Phys. **A 595**, 409, (1995).
- [13] G. Savard, A. Galindo-Uribarri, E. Hagberg, J. C. Hardy, V. T. Koslowsky, D. C. Radford and I. S. Towner, Phys. Rev. Lett. **74**, 1521 (1995).
- [14] H. Behrens and J. Jänecke, Landolt-Bornstein, New Series, Group 1, Vol. **4**, *Numerical Tables for Beta-Decay and Electron Capture*, ed. H. Schopper, Springer-Verlag, Berlin (1969).

[15] Nuclear Data Sheets **60** (1990).

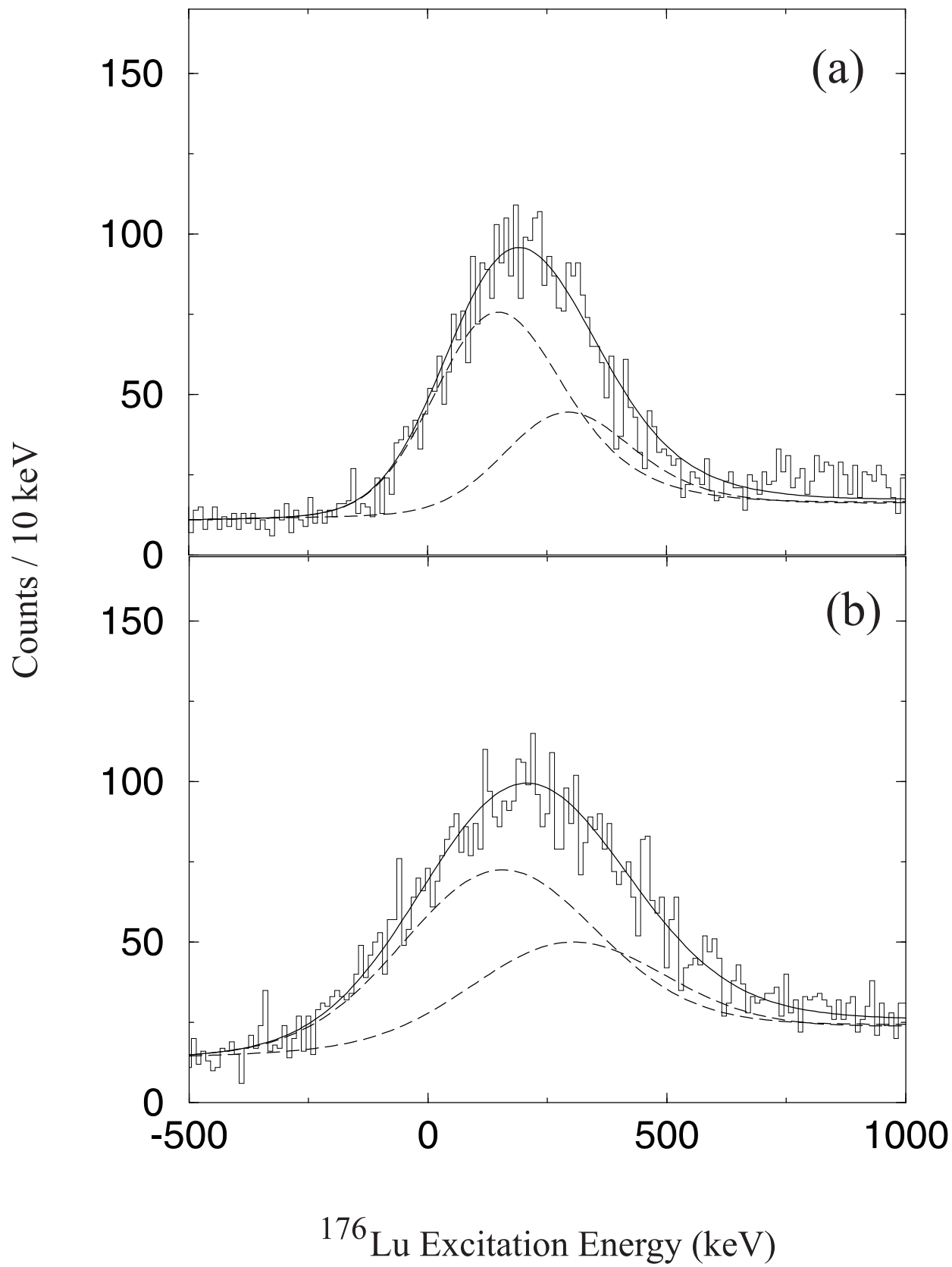


Fig. 1 of A Measurement of GT Strength... by M. Bhattacharya et al.

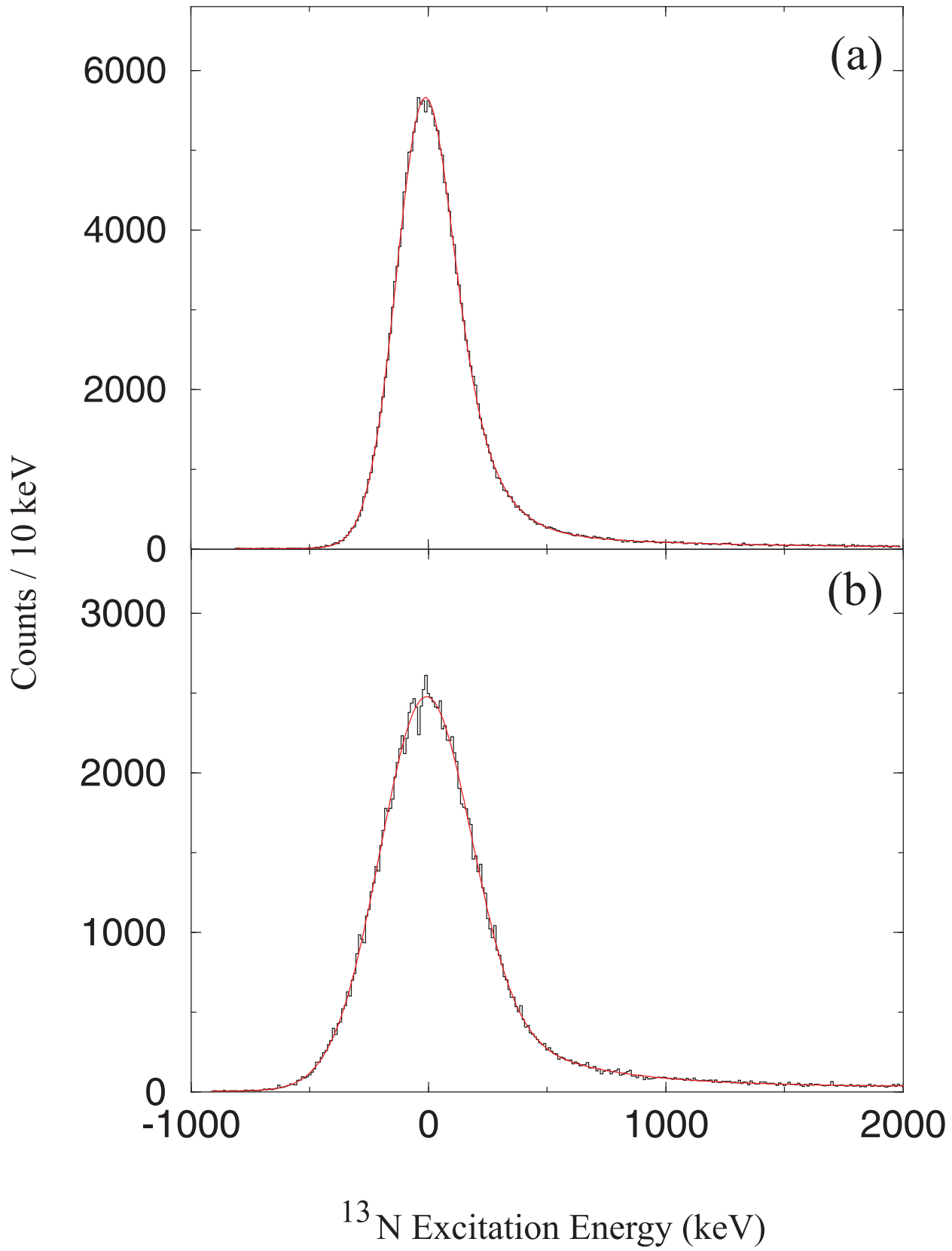


Fig. 2 of A Measurement of GT Strength... by M. Bhattacharya et al.

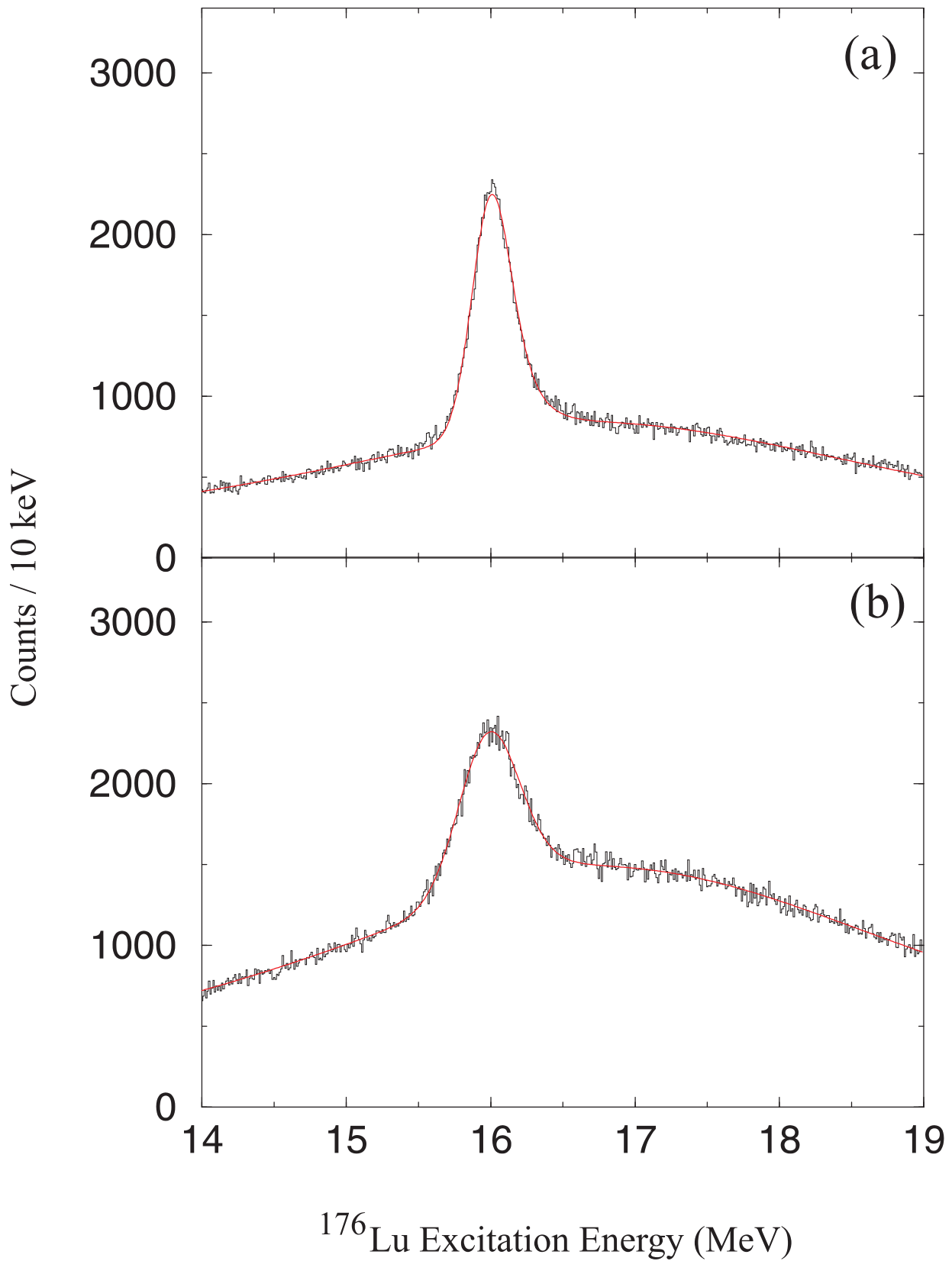


Fig. 3 of A Measurement of GT Strength... by M. Bhattacharya et al.

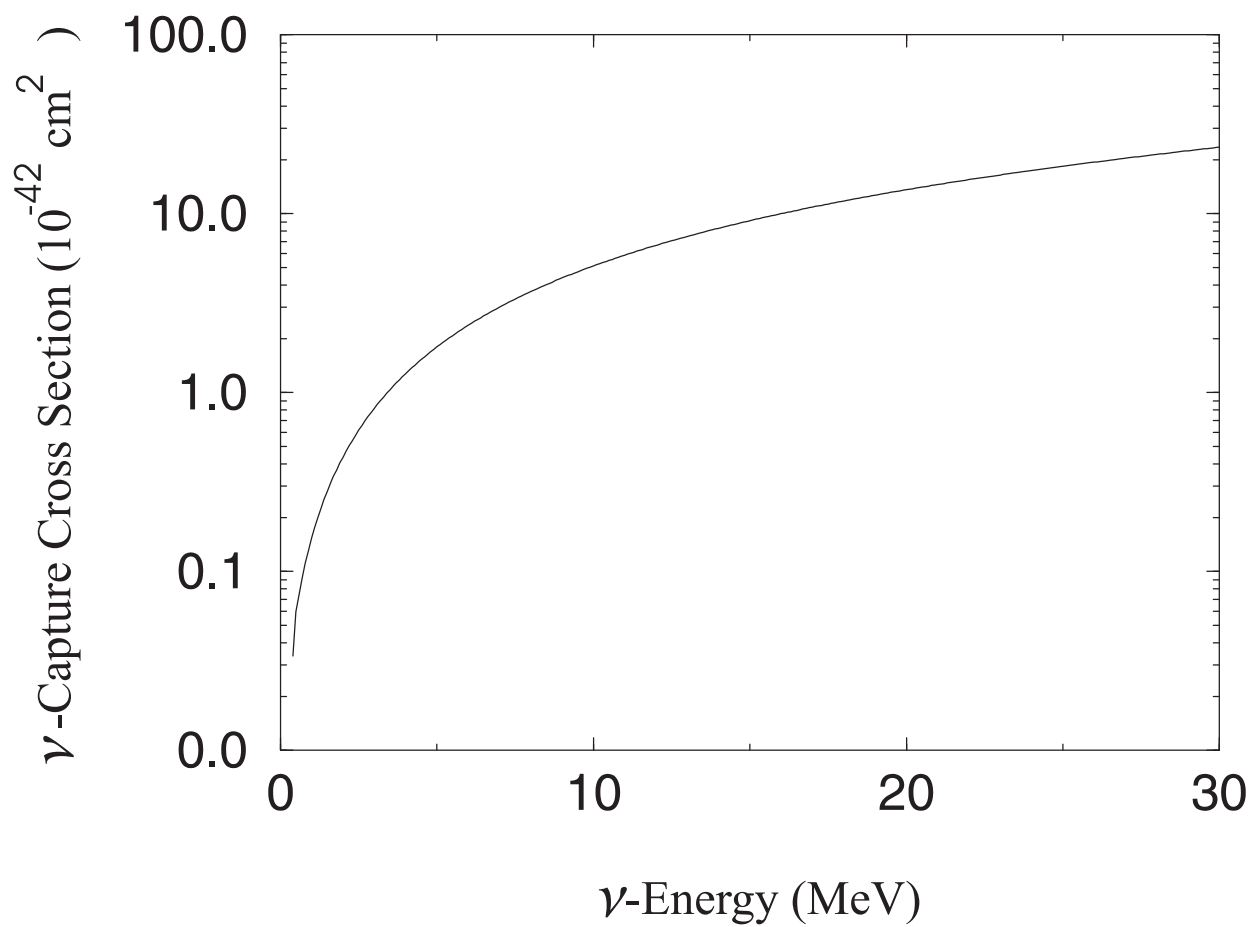


Fig. 4 of A Measurement of GT Strength... by M. Bhattacharya et al.